Physica A 389 (2010) 3299–3306

Contents lists available at ScienceDirect

Physica A

journal homepage: www.elsevier.com/locate/physa

Impact of delays and rewiring on the dynamics of small-world neuronal networks with two types of coupling

Qingyun Wang [a,b,*,1], Matjaž Perc [c], Zhisheng Duan [a], Guanrong Chen [d]

[a] State Key Laboratory for Turbulence and Complex Systems, Department of Mechanics and Aerospace Engineering, College of Engineering, Peking University, Beijing 100871, China

[b] School of Statistics and Mathematics, Inner Mongolia Finance and Economics College, Huhhot 010070, China

[c] Department of Physics, Faculty of Natural Sciences and Mathematics, University of Maribor, Koroška cesta 160, SI-2000 Maribor, Slovenia

[d] Department of Electronic Engineering, City University of Hong Kong, Hong Kong, China

ARTICLE INFO

Article history:
Received 18 February 2009
Received in revised form 15 November 2009
Available online 1 April 2010

Keywords:
Neuronal networks
Gap junctions
Chemical synapses
Information delays
Synchronization transitions

ABSTRACT

We study synchronization transitions and pattern formation on small-world networks consisting of Morris–Lecar excitable neurons in dependence on the information transmission delay and the rewiring probability. In addition, networks formed via gap junctional connections and coupling via chemical synapses are considered separately. For gap-junctionally coupled networks we show that short delays can induce zigzag fronts of excitations, whereas long delays can further detriment synchronization due to a dynamic clustering anti-phase synchronization transition. For the synaptically coupled networks, on the other hand, we find that the clustering anti-phase synchronization can appear as a direct consequence of the prolongation of information transmission delay, without being accompanied by zigzag excitatory fronts. Irrespective of the coupling type, however, we show that an appropriate small-world topology can always restore synchronized activity if only the information transmission delays are short or moderate at most. Long information transmission delays always evoke anti-phase synchronization and clustering, in which case the fine-tuning of the network topology fails to restore the synchronization of neuronal activity.

© 2010 Elsevier B.V. All rights reserved.

1. Introduction

Neuronal networks consist of chemically coupled or functionally associated neurons, whereby the connections among them can be formed by gap junctions or chemical synapses [1]. In the vertebrate cortex, a single neuron can be connected to as many as 10,000 postsynaptic neurons, which in turn leads to the formation of complex networks that can also exhibit small-world properties [2]. Neuronal network dynamics is currently a vibrant topic in theoretical neuroscience [3,4], and indeed, a large body of theoretical works has accumulated focusing specifically on pulse-coupled biological networks [5–7]. Synchronization, pattern formation, and coherence of temporal and spatial neuronal dynamics have also been investigated extensively in recent years [8–11].

Among the array of possible complex dynamical behaviors, synchronization [10] seems to be very important for the efficient processing and transmission of information across the nervous system. One of the coordinating mechanisms in the

* Corresponding author at: School of Statistics and Mathematics, Inner Mongolia Finance and Economics College, Huhhot 010070, China. Tel.: +86 4713812769; fax: +86 4713812769.
E-mail address: nmqingyun@163.com (Q. Wang).
[1] Current address: Department of Dynamics and Control, Beihang University, Beijing 100191, China.

0378-4371/$ – see front matter © 2010 Elsevier B.V. All rights reserved.
doi:10.1016/j.physa.2010.03.031

brain appears to be the synchronization of neuronal activity via phase locking [12]. In the past decade, many theoretical and experimental works have been performed with the aim of analyzing pattern formation and synchronization in an impressive variety of different neuronal networks. Kwon and Moon [13] investigated the effects of small-world connectivity on the phenomenon of coherence resonance in networks of Hodgkin–Huxley neurons. It has been reported that increasing the network randomness may lead to an enhancement of temporal coherence and spatial synchronization. Gong et al. also found that the spatial synchronization and coherence, which are practically absent in regular networks, can be greatly enhanced by random shortcuts between the neurons [14]. Complex spatiotemporal behavior, including in-phase and anti-phase synchronization as well as various wave patterns, has been observed in a ring network of discrete bursting oscillators [15]. Synchronized bursting activity has also been reported [16]. Moreover, the impact of subthreshold pacemaker activity on the dynamics of noisy excitable small-world networks has been investigated in Ref. [17], whereas subthreshold stimulus-aided synchronization and wave formation on a square lattice consisting of discrete Rulkov neurons have been studied in Ref. [18].

As is well known, information transmission delays are inherent to the nervous system because of the finite speed at which action potentials propagate across neuron axons, as well as due to the time lapses occurring by both dendritic and synaptic processing. Typical conduction velocities approximately equal to 10 m/s, leading to non-negligible transmission times, in the order of milliseconds or even hundreds of milliseconds, are needed for information propagation across the cortical network [19]. It is known that different time delay lengths can change both qualitative as well as quantitative properties of the dynamics [20], such as introducing or destroying stable oscillations, enhancing or suppressing synchronization between different neurons, as well as generating complex spatiotemporal patterns. Notably, it has been suggested that time delays can facilitate synchronization among neurons and lead to many interesting and even unexpected phenomena [21,22]. Most recently, it has been found that zigzag fronts of excitations, clustering anti-phase synchronization and in-phase synchronization, can be induced by information transmission delays in map-based neuronal networks [23].

At present, we aim to extend the subject by studying pattern formation and synchronization transitions on small-world Morris–Lecar neuronal networks with two types of coupling. We consider separately gap-junctional and synaptic coupling, both under the influence of different information transmission delays and noise. Thereby we conceptually follow an interesting study by Balenzuela and García-Ojalvo [24], reporting that chemical synapses may be beneficial for the temporal coherence of a coupled neuronal system. We report several non-trivial effects induced by finite delay lengths and small-world topology, such as the emergence of zigzag fronts and clustering anti-phase synchronization transitions. Moreover, we compare the effects of the two considered coupling types on spatiotemporal synchronization and synchronization transitions. Accordingly, the continuation of this paper is organized as follows. Firstly, we introduce the employed neuronal model and other mathematical methods presently in use. Secondly, we present the main results, whereas lastly, we summarize our work and discuss its potential implications.

2. Model description

The spatiotemporal evolution of the studied neuronal network, along with the additive Gaussian noise and information transmission delay, is governed by the following system [25]:

$$\begin{aligned} \frac{dV_i}{dt} &= \frac{1}{C_m}(I_i^{app} - I_i^{ion} - I_i^{syn}) + w\xi_i(t), \\ \frac{dW_i}{dt} &= \phi\Lambda(V_i)\left[W_\infty(V_i) - W_i\right], \end{aligned} \tag{1}$$

where $i = 1, \ldots, N$ index the neurons, whereas V_i and W_i are the membrane potential and the fraction of open potassium channels, respectively. C_m is the membrane capacitance per unit area, which is a measure of the amount of the electric charge stored (or separated) for a given electric potential. I_i^{app} is the externally applied current. The ionic current I_i^{ion} is given by

$$I_i^{ion} = g_{Ca}m_\infty(V_i)(V_i - V_{Ca}) + g_K W_i(V_i - V_K) + g_L(V_i - V_L), \tag{2}$$

where g_{Ca}, g_K and g_L are the normalization constants that determine the maximum possible conductances for Ca^{2+}, K^+, and the ion leakage, respectively. It is worth noting that the constants g_{Ca}, g_K and g_L have different values for channels of different radii [26,27]. He et al. have therefore proposed a modified Morris–Lecar model including the radius of the fiber [27]. Here, however, we consider the normalization as given in Ref. [25]. V_{Ca}, V_K and V_L are the resting potentials of the calcium, potassium and leaking channels, respectively. ϕ is the decay rate of W_i, and we define the following functions of the membrane potential

$$m_\infty(V) = \frac{1}{2}\left[1 + \tanh\left(\frac{V - V_{m_1}}{V_{m_2}}\right)\right], \tag{3}$$

$$W_\infty(V) = \frac{1}{2}\left[1 + \tanh\left(\frac{V - V_{W_1}}{V_{W_2}}\right)\right], \tag{4}$$

$$\Lambda(V) = \cosh\left(\frac{V - V_{W_1}}{2V_{W_2}}\right), \tag{5}$$

Table 1
The values of all parameters that appear in the investigated equations.

The membrane capacitance $C_m = 5$ (μF/cm^2)
Conductance constants (mS/cm^2) $g_{Ca} = 4.0, g_K = 8, g_L = 2.0$
Reversal potentials (mV) $V_{Ca} = 120, V_K = -80, V_L = -60$
Constants (mV) $V_{m_1} = -1.2$, $V_{m_2} = 18$, $V_{W_1} = 2$, $V_{W_2} = 17.4$
The decay rate $(s^{-1})\phi = 1/15$
$I_{app} = 46$

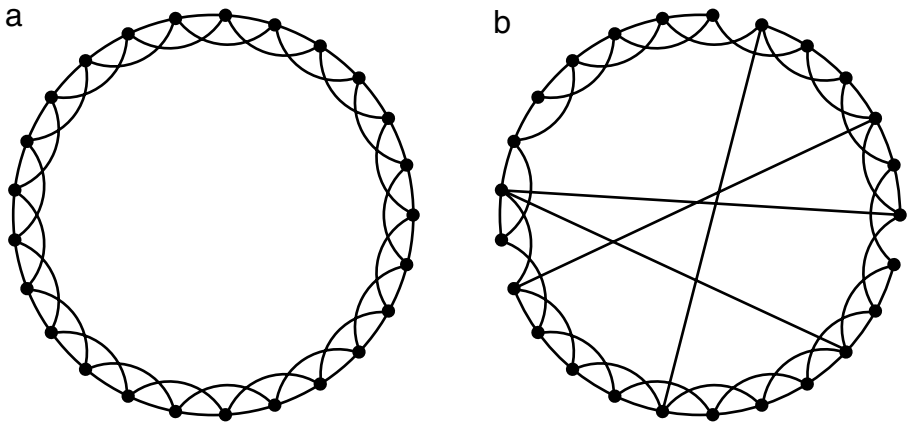

Fig. 1. Examples of considered network topologies. For clarity regarding k and p only 25 vertices are displayed in each panel. (a) Regular ring characterized by $p = 0$ with periodic boundary conditions. Each vertex is connected to its $k = 4$ nearest neighbors. (b) Realization of small-world topology via random rewiring of a certain fraction p of links (in this case 4 out of all 100 were rewired, hence $p = 0.04$).

where V_{m_1}, V_{m_2}, V_{W_1} and V_{W_2} are constants to be specified later. ξ_i is the Gaussian noise in the ith neuron with $\langle \xi_i \rangle = 0$ and $\langle \xi_i(t)\xi_j(t') \rangle = \delta_{i,j}\delta(t - t')$. w is the noise intensity. I_i^{syn} is the synaptic current participating in forming the interaction network among neurons. In neuronal systems there exist two types of synapses (gap junctional and chemical) via which neurons can form networks in order to communicate with one another. To understand the biological functions of these two different types of neuronal networks, we consider two different types of coupling in what follows.

The values of all parameters that appear in the above equations are listed in Table 1.

In the absence of noise, an isolated Morris–Lecar neuron [25] exhibits a bifurcation to a limit cycle for increasing values of I_{app}. This bifurcation can be a saddle-node (type I) or a subcritical Hopf (type II) bifurcation, depending on the choice of other parameter values. We choose the parameters such that the Morris–Lecar neuron exhibits the subcritical Hopf bifurcation. The specific values of the parameters used are shown in Table 1. The equations were integrated using the finite-difference forward-step Heun numerical simulation scheme with a fixed integration step equalling $dt = 0.01$ [28].

Underlying interaction networks hosting the Morris–Lecar neurons were obtained by starting from a regular ring with periodic boundary conditions consisting of $N = 300$ vertices, each having $k = 4$ nearest neighbors, as shown in Fig. 1(a). The parameter p determines the probability of rewiring a link and can occupy any value from the unit interval, whereby $p = 0$ constitutes a regular graph while $p = 1$ results in a random network. For $0 < p < 1$, as exemplified in Fig. 1(b), the resulting network may have small-world properties in that the characteristic path length between distant units is small, i.e. comparable with that of a random network, while the clustering coefficient is still large, i.e. comparable with that of a regular nearest-neighbor graph. The rewiring probability p is one of the main parameters to be varied below. We note that the rewiring probability p can be considered as a tunable homotopy-like parameter [29] between 0 and 1, i.e. when $p = 0$ the graph is not rewired whilst when $p = 1$ the graph is rewired at random thus resulting in a random network.

3. The two coupling types

In the following, we describe the modeling of the two coupling types. Particularly, gap-junctional coupling with information transmission delay can be described as follows:

$$I_i^{\text{syn}} = g^{\text{syn}} \sum_j \varepsilon_{i,j} \left[V_i(t) - V_j(t - \tau) \right]. \tag{6}$$

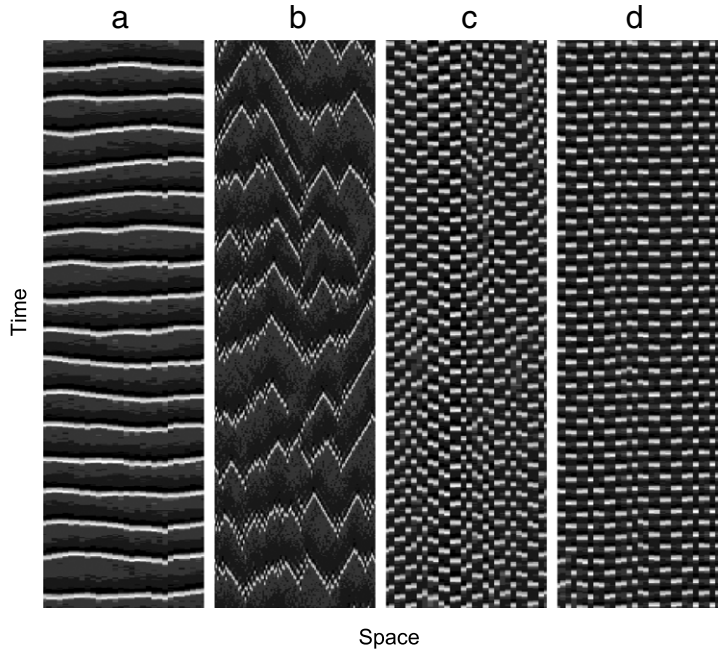

Fig. 2. Space–time plots obtained for different information transmission delays. From left to right τ equals 0, 4.8, 10 and 12, respectively. Other parameter values are $p = 0.1$ and $w = 2.5$. It can be observed that the excitations converge to clustering anti-phase synchronization as the delay increases.

The coupling strength in this case is set to $g^{\text{syn}} = 0.5$ throughout this work, whereby $\varepsilon_{i,j} = 1$ if neuron i is coupled to neuron j, while $\varepsilon_{i,j} = 0$ otherwise. Finally, τ is the information transmission delay, which will be one of the main parameters to be varied below.

In order to take into account the chemical nature of the synapses, we use the model proposed in Ref. [24] to capture the essence of synaptic coupling among the neurons. In this model, the synaptic current through the ith neuron is given by

$$I_i^{\text{syn}} = g^{\text{syn}} \sum_j r_j(t-\tau)\,[V_i(t) - E_s]\,, \tag{7}$$

where the sum runs over the neighbors that feed the ith neuron, D is the conductance of the synaptic channel, r_j represents the fraction of bound receptors, V_i is the postsynaptic membrane potential, and E_s is a parameter whose value determines the type of the synapse (if larger than the rest potential, *e.g.* $E_s = 0$ mV, the synapse is excitatory; if smaller, *e.g.* $E_s = -80$ mV, it is inhibitory). τ is the information transmission delay. The fraction of bound receptors, r_j, follows the equation

$$\frac{\mathrm{d}r_j}{\mathrm{d}t} = \alpha[T]_j(1 - r_j) - \beta r_j, \tag{8}$$

where $[T]_j = T_{\max}\theta(T_0^j + \tau_{\text{syn}} - t)\theta(t - T_0^j)$ is the concentration of neurotransmitter released into the synaptic cleft, α and β are rise and decay time constants, respectively, and T_0^j is the time at which the presynaptic neuron j fires, which happens whenever the presynaptic membrane potential exceeds a predetermined threshold value. In our case, the later is chosen to be 10 mV. This threshold mechanism lies at the origin of the nonlinear character of the chemical synaptic coupling, which contrasts with the linear nature of the diffusive electrical coupling of Eq. (6). The time during which the synaptic connection is active is given by τ_{syn}. The values of parameters related to the synaptic coupling are $g^{\text{syn}} = 1, \alpha = 2.0, \beta = 1.0, T_{\max} = 1.0$, $\tau_{\text{syn}} = 1.5$ and $Es = 0.0$.

4. Synchronization transitions in neuronal networks with gap-junctional coupling

In what follows, we present the effects of information transmission delay (τ) and the rewiring probability (p) on pattern formation and synchronization in neuronal networks with gap-junctional coupling. Results presented in Fig. 2 illustrate the spatiotemporal dynamics of neurons that is evoked by different values of τ on a typical realization of small-world topology emerging at $p = 0.1$. In the absence of information transmission delay the neurons can synchronize their spiking activity, as illustrated in Fig. 2(a). By non-zero yet short delays, zigzag fronts of excitations appear, as shown in Fig. 2(b), leading to the loss of spiking synchronization. In Fig. 2(c), however, it is illustrated that further increasing the delay can induce alternative layer patterns, at which excitatory spikes appear alternatively among nearby clusters in space as the temporal dynamics evolves. Hence, this phenomenon can be termed appropriately as a clustering anti-phase synchronization transition induced by an appropriate information transmission delay. Moreover, for larger values of τ the clustering anti-phase synchronization

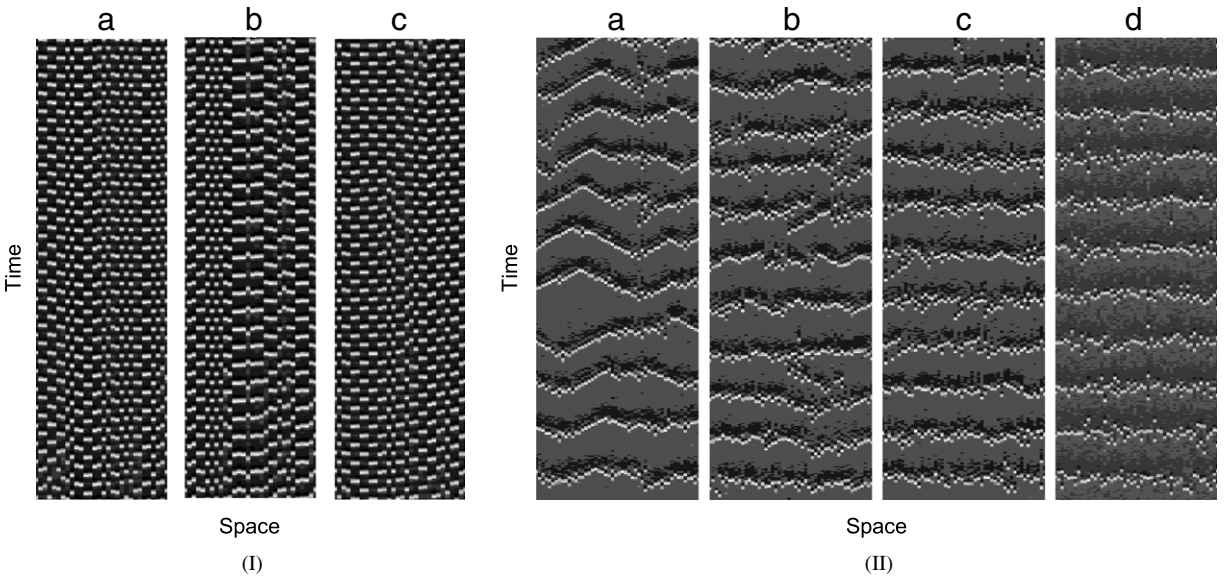

Fig. 3. (I) Space–time plots obtained for different rewiring probabilities. From left to right p equals 0.063, 0.35 and 0.8, respectively. The delay is $\tau = 10$. It can be observed that as p increases, clustering anti-phase synchronization always persists for large delays. (II) Space–time plots obtained for different rewiring probabilities. From left to right p equals 0.1, 0.4, 0.6 and 0.8, respectively. Delay is $\tau = 4.8$. It can be observed that as p increases, in-phase synchronization can be restored for short delays.

can also be observed [see Fig. 2(d)], appearing even more consistently as by shorter delays. More interestingly, we find that for short delays less spikes are fired in a given time interval, and consequently, the frequency of neuronal firings decreases. Further increasing the delay leads to more spikes, thus correspondingly increasing the frequency of neuronal firings. In fact, this is understandable since the delay introduces phase slips, and hence zigzag fronts and alternative layer patterns can appear, thus supplementing the purely noise-induced excitations. It can indeed be concluded that the information transmission delay plays a pivotal role by the generation of spatiotemporal patterns and synchronization in networked neuronal systems.

Next, we visually inspect the impact of different values of p on the synchronization within the studied system with a finite information transmission delay. To do so, we set $\tau = 10$ and $w = 2.5$, and subsequently vary p. The results in the form of space–time plots are presented in Fig. 3(I). It can be observed that as p increases the clustering anti-phase synchronization always persists with only a little difference among the clusters evoked by different values of p. On the other hand, for short delays, *e.g.* $\tau = 4.8$, as p increases the zigzag fronts of excitations gradually vanish and give way to near-regular in-phase synchronization, as shown in Fig. 3(II). The synchronization seems to saturate as p is enlarged towards the random network limit. Notably, we do not observe clustering anti-phase synchronization as reported above, which leads us to the conclusion that the clustering anti-phase synchronization is a consequence of a suitable information transmission delay rather than complex, or small-world in particular, network topology. For other delay lengths we have conducted similar investigations, and found that for short delays the suitable rewiring probability can restore in-phase synchronization. The clustering anti-phase synchronization, however, is independent of network topology for long information transmission delays.

To study the above observations, and in particular the degree of synchronization, quantitatively, we introduce a synchronization parameter σ by means of the standard deviation [30] as follows:

$$\sigma = \frac{1}{T}\int_0^T \sigma(t)\mathrm{d}t, \qquad \sigma(t) = \frac{1}{N}\sum_{j=1}^{N}[V^j(t)]^2 - \left[\frac{1}{N}\sum_{j=1}^{N}V^j(t)\right]^2, \tag{9}$$

where T is the period of numerical integration. In particular, σ is a suitable quantity for numerically effectively measuring the spatial synchronization of excitations, hence revealing different synchronization regions and related synchronization transitions.

As shown in Fig. 4, we plot σ versus τ for different values of p. It can be seen that, as the delay increases, σ initially decreases. However, this cannot imply the enhancement of spiking synchronization. On the contrary, spiking synchronization is destroyed from the above observations. In fact, it can be seen that for short delays, zigzag fronts can appear, which destroys synchronization. Decreasing the spiking frequency results in a smaller synchronization parameter σ. With delays being increased further, clustering anti-phase synchronization can be observed since σ becomes large. We have conducted detailed investigations and found zigzag fronts for the small delays and anti-phase synchronization of nearby clusters for the large values of τ. In Fig. 4(b), σ is presented in dependence on p for different values of τ. Evidently, for smaller delays σ clearly decreases past the small-world topology. For the intermediate delays, σ retains intermediate values, which

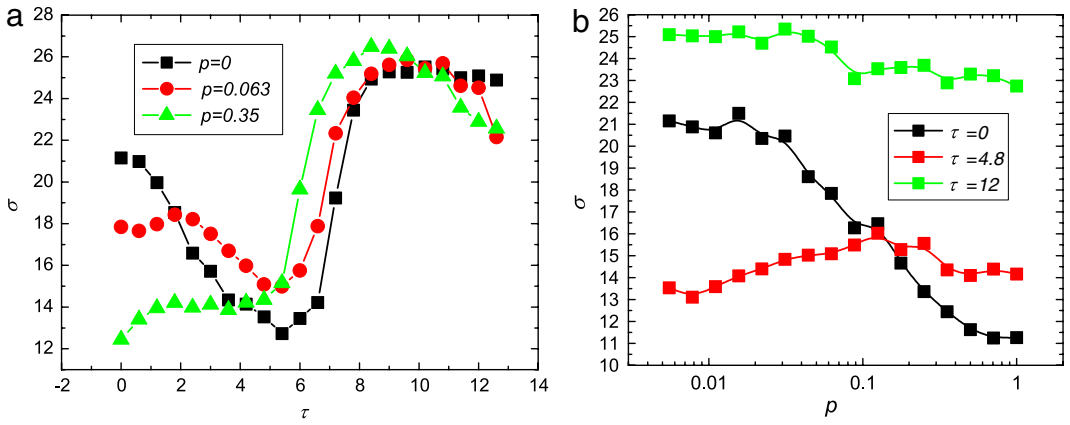

Fig. 4. (a) Dependence of the synchronization parameter σ on τ for different values of p. (b) Dependence of σ on p for different values of τ; wherever applicable, other parameters are the same as in Fig. 2.

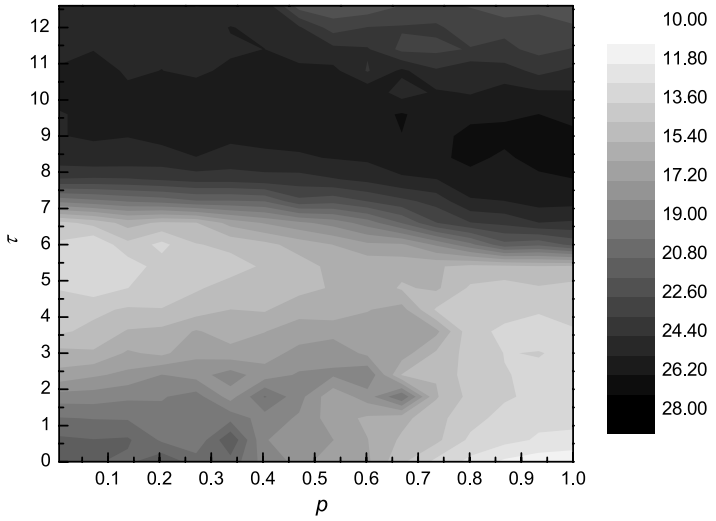

Fig. 5. Contour plots of σ in dependence on p and τ, showing the transitions to different synchronization regions (see also the main text for details). Other parameters are the same as in Fig. 2.

change much less profoundly as p is increased. Further investigations have shown that for the case of intermediate delays the zigzag fronts can transit to near regular synchronization and finally saturate as p approaches the random network limit. For the large delays the impact of different values of p on σ is also much less profound, and σ keeps on the larger values, suggesting that the clustering anti-phase synchronization is robust against alterations of the interaction network.

To make an overall inspection, the dependence of σ on both p and τ is presented in Fig. 5 with the noise level equalling $w = 2.5$. It is evident that for the smaller delays neurons can transit to more regular synchronization as p increases. For the intermediate and larger delays, however, σ undergoes no significant changes as p increases, which corresponds to the above-detailed analysis. We can thus conclude that both p and τ have a non-trivial impact on spatial synchronization in noisy neuronal networks.

5. Synchronization transitions in neuronal networks with synaptic coupling

In this section, we examine the impact of information transmission delay and rewiring probability on the spatiotemporal synchronization in small-world neuronal networks with chemical synapses. Numerical results presented in Fig. 6 illustrate the spatiotemporal dynamics of neurons evoked by different values of τ on a typical realization of small-world topology emerging for $p = 0.1$. It can be seen that in the absence of information transmission delay, neurons can almost synchronize their spiking, as shown in Fig. 6(a). As the delay increases, the neuronal excitations converge to a clustering anti-phase synchronization, as shown in Fig. 6(b) and (c). Further investigations show that no zigzag fronts of excitations can appear for short delays, which is different from the case of gap-junctional coupling. Comparing the two considered coupling types, it can be concluded that delays can have a different impact on the spatiotemporal pattern formation and synchronization in neuronal networks.

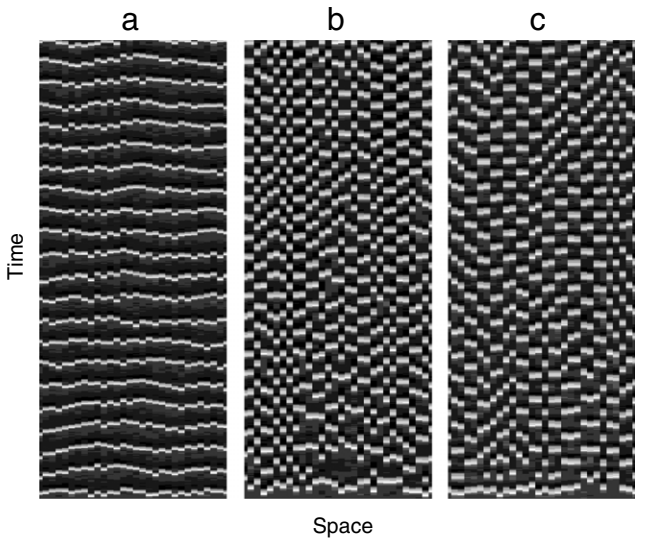

Fig. 6. Space–time plots obtained for different information transmission delays, evidencing the transition to clustering anti-phase synchronization as the delay is increased. From left to right τ equals 0, 4.8 and 10, respectively. Other parameter values are $p = 0.1$ and $w = 2.5$.

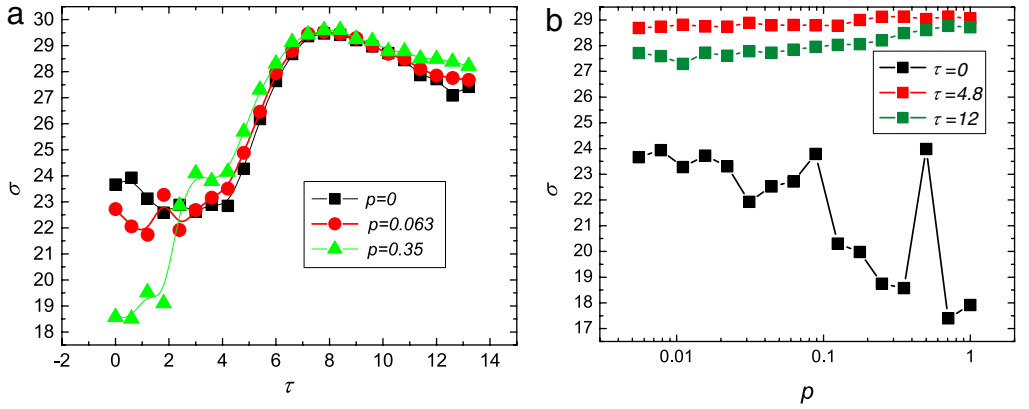

Fig. 7. (a) Dependence of the synchronization parameter σ on τ for different values of p. (b) Dependence of σ on p for different values of τ; wherever applicable, other parameters are the same as in Fig. 6.

Similarly, results of σ versus τ are shown in Fig. 7(a) for different p. It can be seen that, as the delay increases, σ also increases, which suggests the loss of spiking synchronization. Consequently, the clustering anti-phase synchronization appears. With delays being increased further, σ becomes somewhat smaller, yet the clustering anti-phase synchronization still persists. Fig. 7(b) presents the variation of σ as p is changed for different values of τ. Evidently, for smaller delays σ clearly decreases at some suitable values of p. For the intermediate and larger delays, however, σ practically retains a constant value, thus implying no clear impact of small-world topology on synchronization of neuronal networks with synaptic coupling. An overall inspection of σ on both p and τ is presented in Fig. 8, which fully supports our above assessment.

6. Summary

The different characters of gap junction and chemical coupling are explored in terms of pattern formation and synchronization of the neuronal network as the information transmission delay and rewiring probability are varied. It is found that, for the gap-junctional coupling, if the delay is short or moderate, neurons within the network can exhibit transitions from zigzag fronts to clustering anti-phase synchronization. Moreover, we show that spatial zigzag fronts can transit to increasingly regular in-phase synchronization as p closes to the limit constituting random networks. For large delays, however, the clustering anti-phase synchronization is independent from the network topology. For chemical synapses, delays can make neurons transit directly from spiking synchronization to clustering anti-phase synchronization. Then, for the case of short delays, a suitable rewired network topology can enhance the synchronization of excitations in neuronal networks.

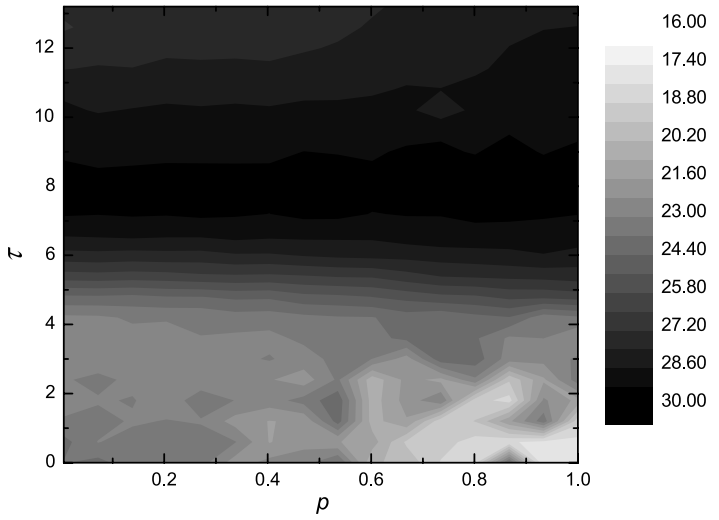

Fig. 8. Contour plots of σ in dependence on p and τ, depicting the transitions to different synchronization regions (see also the main text for details). Other parameter values are the same as in Fig. 6.

Synapses in neuronal systems are one of the most important means through which neurons form the specialized network structures. It is well known, however, that both, chemical synapses as well as gap junctions, play a significant role in assuring robust information processing within the brain. Thus, although previous works have been largely concerned with gap-junctional coupling, we emphasize that the role of chemical synapses has to be studied in detail as well, especially when examining spatiotemporal dynamics and synchronization within neuronal networks. The present study aims towards achieving this goal, and we hope that it will serve as a useful guide for understanding the role of chemical synapses in the dynamics of neuronal systems.

Acknowledgements

This work was supported by the National Science Foundation of China (Fund Nos. 10972001, 10702023 and 10832006) and China's Post-Doctoral Science Foundation (Fund No. 200801020). Matjaž Perc additionally acknowledges support from the Slovenian Research Agency (Fund No. Z1-2032-2547).

References

[1] M.A. Arbib (Ed.), The Handbook of Brain Theory and Neural Networks, MIT Press, Massachusetts, 1995.
[2] D.J. Watts, S.H. Strogatz, Nature 393 (1998) 440.
[3] H.D.I. Abarbanel, M.I. Rabinovich, A. Selverston, M.V. Bazhenov, R. Huerta, M.M. Suschchik, L.L. Rubchinskii, Phys. Usp. 39 (1996) 337.
[4] M.I. Rabinovich, P. Varona, A.I. Selverston, H.D.I. Abarbanel, Rev. Modern Phys. 78 (2006) 1213.
[5] N. Brunel, D. Hansel, Neural Comput. 18 (2006) 1066.
[6] N. Brunel, J. Physiol. Paris 94 (2000) 445.
[7] W.M. Kistler, W. Gerstner, Neural Comput. 14 (2002) 987–997.
[8] J.F. Lindner, B.K. Meadows, W.L. Ditto, M.E. Inchiosa, A.R. Bulsara, Phys. Rev. Lett. 75 (1995) 3.
[9] C. Zhou, J. Kurths, B. Hu, Phys. Rev. Lett. 87 (2001) 098101.
[10] A. Pikovsky, M. Rosenblum, J. Kurths, Synchronization: A Universal Concept in Nonlinear Sciences, Cambridge University Press, Cambridge, 2001.
[11] Q.Y. Wang, Z.S. Duan, L. Huang, G.R. Chen, Q.S. Lu, New J. Phys. 9 (2007) 383.
[12] T. Pereira, M.S. Baptista, J. Kurths, Europhys. Lett. 77 (2007) 40006.
[13] O. Kwon, H.-T. Moon, Phys. Lett. A 298 (2002) 319.
[14] Y.B. Gong, B. Xu, Q. Xu, C.L. Yang, T.Q. Ren, Z.H. Hou, H.W. Xin, Phys. Rev. E 73 (2006) 046137.
[15] G. Tanakaa, B. Ibarz, M.A.F. Sanjuan, K. Aihara, Chaos 16 (2006) 013113.
[16] Q.Y. Wang, Q.S. Lu, G.R. Chen, Physica A 374 (2007) 869.
[17] M. Perc, Phys. Rev. E. 76 (2007) 066203.
[18] Q.Y. Wang, Q.S. Lu, G.R. Chen, Europhys. Lett. 77 (2007) 10004.
[19] E.R. Kandel, J.H. Schwartz, T.M. Jessell, Principles of Neural Science, Elsevier, Amsterdam, 1991.
[20] A. Roxin, N. Brunel, D. Hansel, Phys. Rev. Lett. 94 (2005) 238103.
[21] Q.Y. Wang, Q.S. Lu, Chin. Phys. Lett. 3 (2005) 543.
[22] E. Rossoni, Y.H. Chen, M.Z. Ding, J.F. Feng, Phys. Rev. E 71 (2005) 061904.
[23] Q.Y. Wang, Q.S. Lu, G.R. Chen, Europhys. Lett. 78 (2008) 50008.
[24] P. Balenzuela, J. García-Ojalvo, Phys. Rev. E 72 (2005) 021901.
[25] C. Morris, H. Lecar, Biophys. J. 35 (1981) 193.
[26] J.H. He, Neurosci. Lett. 373 (2005) 48.
[27] J.H. He, X.H. Wu, Neurocomputing 64 (2005) 543.
[28] J. Garcia-Ojalvo, J.M. Sancho, Noise in Spatially Extended Systems, Springer, New York, 1999.
[29] M.A. Noor, S.T. Mohyud-Din, Int. J. Nonlinear Sci. Numer. Simul. 9 (2008) 395.
[30] Z. Gao, B. Hu, G. Hu, Phys. Rev. E 65 (2001) 016209.